Electronic Supplementary Information

Highly stable Ni(II)/Zn(II)-CPs as multiresponsive luminescent sensors for detection of IO_4^-, 2,6-dichloro-4-nitrophenol and folic acid

Fang-Hua Zhao*, Zi-Hao Zhao, Rui Feng, Yu-Shuo Li, Shu-Qi Li, Zhi-Hong Jing, Zhong-Lin Li*

Key Laboratory of Life-Organic Analysis of Shandong Province, School of Chemistry and Chemical Engineering, Qufu Normal University, Qufu 273165, China.

*Corresponding author. Email: zfh101@163.com (F-H. Zhao); lizhonglin788@163.com (Z.-L. Li)

Table S1. Crystal data and structure refinements for **1** and **2**

Identification code	**1**	**2**
Empirical formula	$C_{110}H_{150}N_{16}O_{19}Ni_3$	$C_{30}H_{40}N_4O_5Zn$
Formula weight	2176.58	602.03
Temperature/K	153(2)	153(2)
Crystal system	Triclinic	Triclinic
Space group	*P*-1	*P*-1
a (Å)	9.6380(6)	8.6275(6)
b (Å)	16.3649(10)	11.5489(9)
c (Å)	17.7092(11)	16.2320(13)
α (°)	77.012(3)	108.870(2)
β (°)	87.238(3)	93.870(3)
γ (°)	79.995(3)	109.641(4)
V (Å^3)	2680.2(3)	1421.03(19)
Z	1	2
ρ_{calc} (g/cm^3)	1.349	1.407
μ/mm^{-1}	0.597	0.911
R_{int}	0.0510	0.0720
Reflections collected	46525	24787
Data/restraints/parameters	10514/1/676	5587/0/364
Goodness-of-fit on F^2	1.015	1.009
Final R indexes [$I > 2\sigma$(I)]	R_1 = 0.0493 wR_2 = 0.1205	R_1 = 0.0418 wR_2 = 0.0798
Final R indexes [all data]	R_1 = 0.0792 wR_2 = 0.1393	R_1 = 0.0700 wR_2 = 0.0900
Largest diff. peak/hole/e Å^{-3}	1.03/-0.5	0.37/-0.34
CCDC	2348596	2348597

Table S2. Bond Lengths (Å) and Bond Angles (°) for **1** and **2**.

1	N1–Ni1	2.138(2)	N7–Ni1	2.152(2)	Ni1–O2	2.157(2)
	N3–Ni2	2.065(2)	Ni1–O5	2.017(2)	Ni2–O4	2.100(2)
	N5–Ni1	2.087(3)	Ni1–O1	2.1107(19)	Ni2–O4^5	2.100(2)
	Ni2–O3^5	2.142(2)	Ni2–O3	2.142(2)	O5–Ni1–N5	87.90(10)
	O5–Ni1–O1	169.79(9)	N3–Ni2–N3^6	180	O4^6–Ni2–O3^6	61.93(8)
	N5–Ni1–O1	102.28(9)	N3^6–Ni2–O4	89.04(8)	O4–Ni2–O3^6	118.07(8)
	O5–Ni1–N1	92.14(9)	N3–Ni2–O4	90.96(8)	O3–Ni2–O3	180
	N5–Ni1–N1	87.63(9)	N3^6–Ni2–O4^6	90.96(8)	N1–Ni1–O2	89.71(8)
	O1–Ni1–N1	89.11(8)	N3–Ni2–O4^6	89.04(8)	N7–Ni1–O2	87.35(8)
	O5–Ni1–N7	88.62(9)	O4^6–Ni2–O4	180	N5–Ni1–O2	164.00(9)
	N5–Ni1–N7	95.24(9)	N3^6–Ni2–O3^6	90.18(9)	O1–Ni1–O2	61.89(8)
	O1–Ni1–N7	89.64(8)	N3^6–Ni2–O3	89.83(9)	N3–Ni2–O3^6	89.83(9)
	N1–Ni1–N7	177.06(9)	O4^6–Ni2–O3	118.07(8)	N3–Ni2–O3	90.17(9)
	O5–Ni1–O2	107.98(9)	O4–Ni2–O3	61.93(8)		
2	N1–Zn1	2.007(2)	N5–Zn1	2.006(2)	O1–Zn1	1.9551(19)
	O3–Zn1	1.973(2)	O3–Zn1–N5	101.72(9)	O3–Zn1–N1	102.00(9)
	O1–Zn1–O3	115.61(8)	O1–Zn1–N1	102.64(9)	N5–Zn1–N1	118.68(9)
	O1–Zn1–N5	115.92(9)				

1: ^{1}-1+X,-1+Y,1+Z; ^{2}2-X,1-Y,1-Z; ^{3}1-X,1-Y,1-Z; ^{4}2-X,2-Y,-Z; ^{5}3-X,2-Y,-1-Z. ^{1}-1+X,-1+Y,1+Z; ^{2}1+X,1+Y,-1+Z; ^{3}2-X,1-Y,1-Z; ^{4}1-X,1-Y,1-Z; ^{5}2-X,2-Y,-Z; ^{6}3-X,2-Y,-1-Z.
2: ^{1}2-X,1-Y,2-Z; ^{2}1-X,-1-Y,1-Z; ^{3}3-X,1-Y,2-Z; ^{4}2-X,-1-Y,1-Z. ^{1}2-X,1-Y,2-Z; ^{2}1-X,-1-Y,1-Z; ^{3}3-X,1-Y,2-Z; ^{4}2-X,-1-Y,1-Z.

Table S3. Hydrogen Bond Lengths (Å) and Bond Angles (°) for **1** and **2**

	D–H···A	d(D–H)	d(H···A)	d(D···A)	∠(D–H···A)
	O9–H9D···O6[3]	0.86	1.94	2.789(4)	166
	O9–H9C···O4[6]	0.86	1.94	2.754(3)	159
	O8–H8D···O3[5]	0.85	1.99	2.823(3)	162.8
	O8–H8C···O9[3]	0.85	1.96	2.815(3)	173
	O7–H7D···O8	0.86	2.09	2.890(4)	155.6
	O7–H7C···O6	0.87	1.97	2.833(4)	173.3
	C54–H54···O8[4]	0.95	2.43	3.222(4)	140.4
	C51–H51···O10	0.95	2.6	3.473(7)	153
	C49–H49···O7	0.95	2.36	3.180(4)	144.4
	C49–H49···O5	0.95	2.23	2.801(4)	117.5
1	C48–H48A···O7	0.99	2.62	3.470(5)	143.4
	C43–H43B···O9[3]	0.99	2.64	3.564(4)	155.5
	C38–H38···O1	0.95	2.41	3.114(4)	130.4
	C36–H36···O5	0.95	2.48	2.981(4)	112.7
	C34–H34···O9	0.95	2.51	3.412(4)	158.1
	C29–H29···O6	0.95	2.47	3.194(4)	132.7
	C28–H28B···O6[2]	0.99	2.61	3.464(4)	144.1
	C18–H18···O5	0.95	2.59	3.288(4)	130.5
	C16–H16···O10[1]	0.95	2.36	3.061(6)	130
	C16–H16···O1	0.95	2.48	2.966(3)	111.5
	C12–H12B···O2	0.99	2.46	3.412(4)	160.2
	C11–H11···O5[1]	0.95	2.21	3.054(3)	147.8
2	C18–H18B···O3[2]	0.99	2.63	3.597(4)	165.3
	C23–H23A···O4[1]	0.99	2.49	3.425(4)	157.3
	C29–H29···O2[3]	0.95	2.24	3.176(4)	166.2

1: [1]2-X,1-Y,-Z; [2]2-X,2-Y,-Z; [3]1-X,1-Y,1-Z; [4]1-X,2-Y,-Z; [5]-1+X,+Y,1+Z; [6]-1+X,-1+Y,1+Z.
2: [1]1+X,+Y,+Z; [2]2-X,-Y,2-Z; [3]2-X,-Y,1-Z.

Table S4. Comparison of materials for IO_4^- detection.

Material	Methods	Medium	K_{sv}/M^{-1}	LOD/M	Ref.
Zn-DBD-SA	Turn-off	Water	2.46×10^4	6.36×10^{-8}	57
$[Zn_2L2(H_2O)_4]\cdot H_2O$	Turn-on	Water	2.34×10^5	3.8×10^{-8}	58
$\{Ni_3(seb)_3(bbimh)_4\cdot 7H_2O\}_n$ (**1**)	Turn-off	Water	8.52×10^4	1.23×10^{-6}	This work
$\{Zn(seb)(bbimh)\cdot H_2O\}_n$ (**2**)	Turn-off	Water	8.31×10^4	1.26×10^{-6}	This work

Table S5. Comparison of materials for FA detection

Material	Methods	Medium	K_{sv} / M^{-1}	LOD / M	Ref.
$[EuZn(LZ)_2(HCOO)(H_2O)_3]_n$	Turn-on	Water	3.94×10^5	1.84×10^{-8}	59
Eu(HDPB)(phen)	Turn-off	Water	3.44×10^4	1.55×10^{-6}	60
$[Eu_{0.06}Tb_{0.04}Gd_{0.9}(HDPNC)_{1.5}(H_2O)(DMF)]_2\cdot H_2O$	Turn-on	Water	4.35×10^5	8.83×10^{-8}	61
$\{[(CH)_2NH_2]_3[RE_2(BTDBA)_2(HCOO)]\cdot 5H_2O\cdot 2DMF\}_n$	Turn-off	Water	—	2×10^{-5}	62
$[Eu(ppda)(bpdc)_{0.5}(C_2H_5OH)(H_2O)]_n$	Turn-off	Water	—	3.28×10^{-8}	63
$\{[Ni_3(seb)_3(bbimh)_4]\cdot 7H_2O\}_n$ (**1**)	Turn-off	Water	1.38×10^4	1.30×10^{-5}	This work
$\{[Zn(seb)(bbimh)]\cdot H_2O\}_n$ (**2**)	Turn-off	Water	6.69×10^3	1.57×10^{-5}	This work

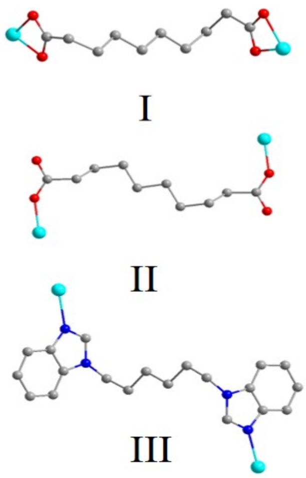

Scheme S1. The coordination modes of seb^{2-} and bbimh in **1** and **2**.

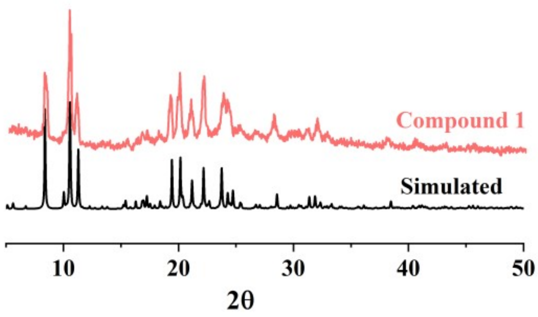

(a)

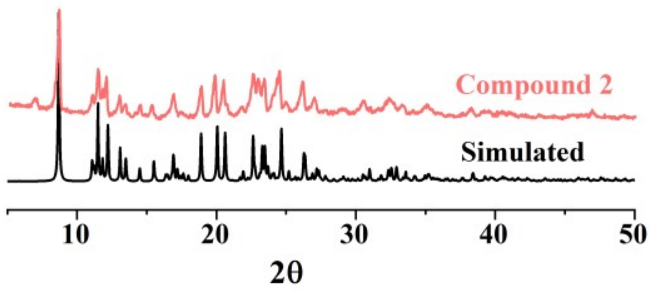

(b)

Fig. S1. (a) and (b) The simulated and experimental PXRD patterns of **1** and **2**.

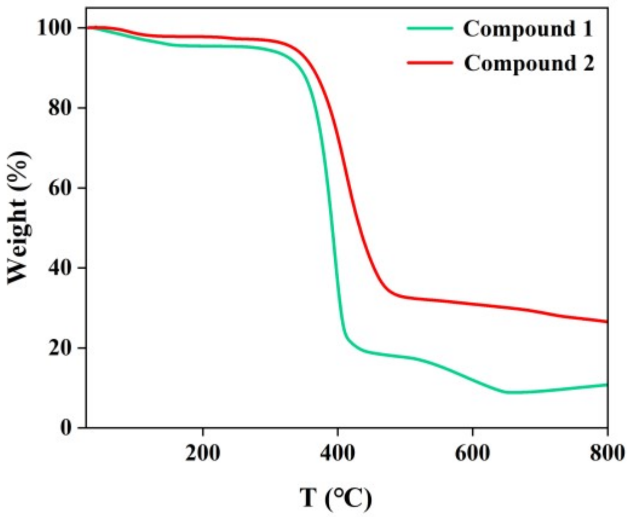

Fig. S2. The TGA curves of **1** and **2**.

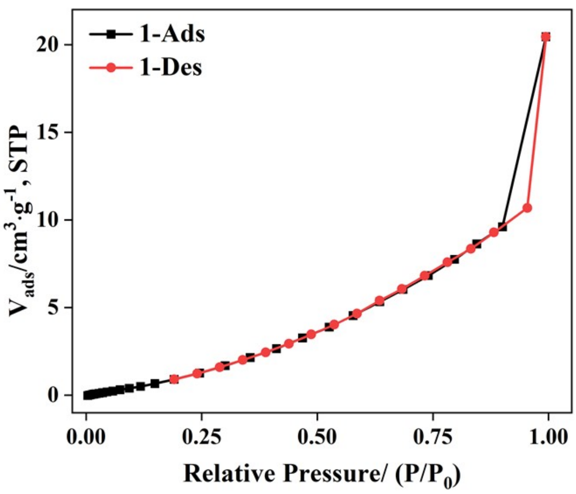

(a)

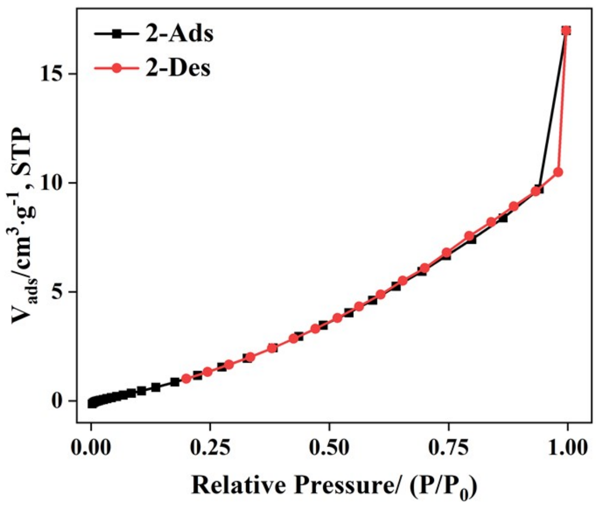

(b)

Fig. S3. The N2 adsorption/desorption isotherms of **1** (a) and **2** (b).

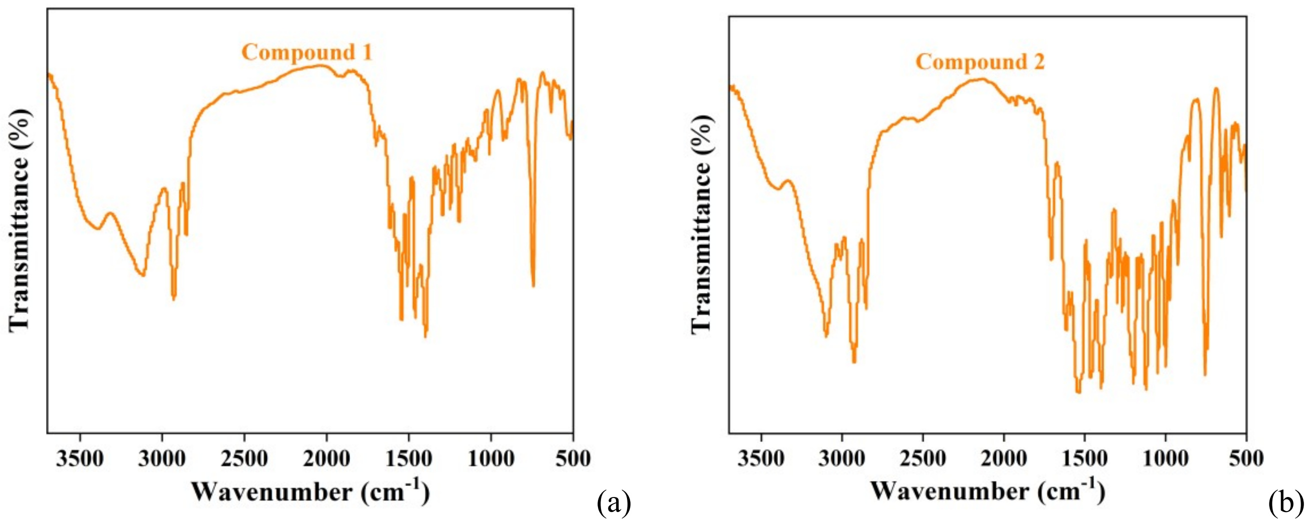

Fig. S4. The IR spectra of **1** and **2**.

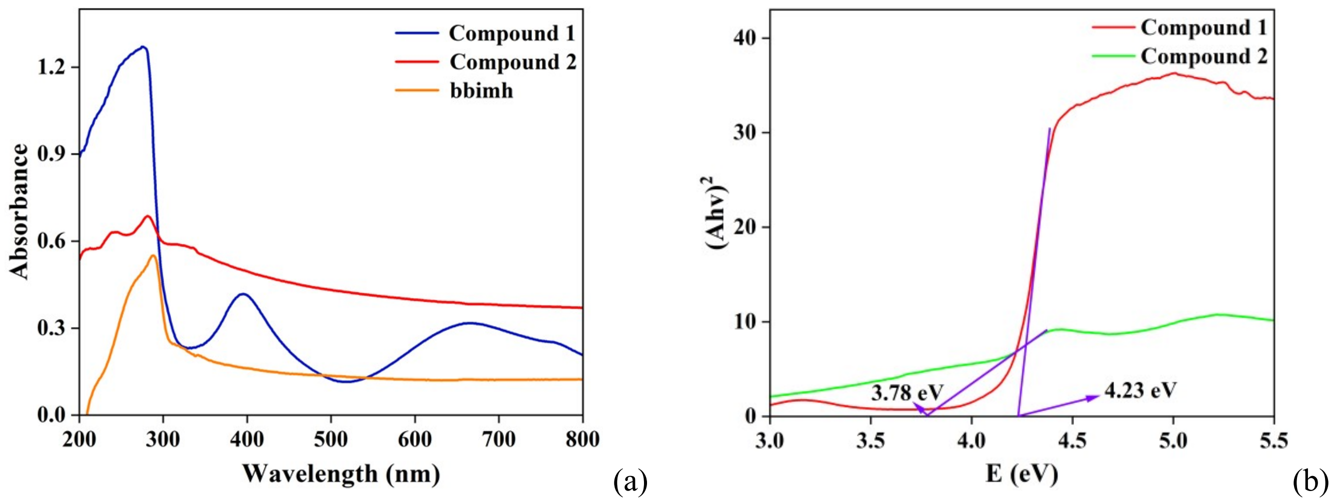

Fig. S5. (a) The solid UV-visible absorption spectra of **1**, **2** and bbimh. (b) Diffuse reflectance spectra of **1** and **2**.

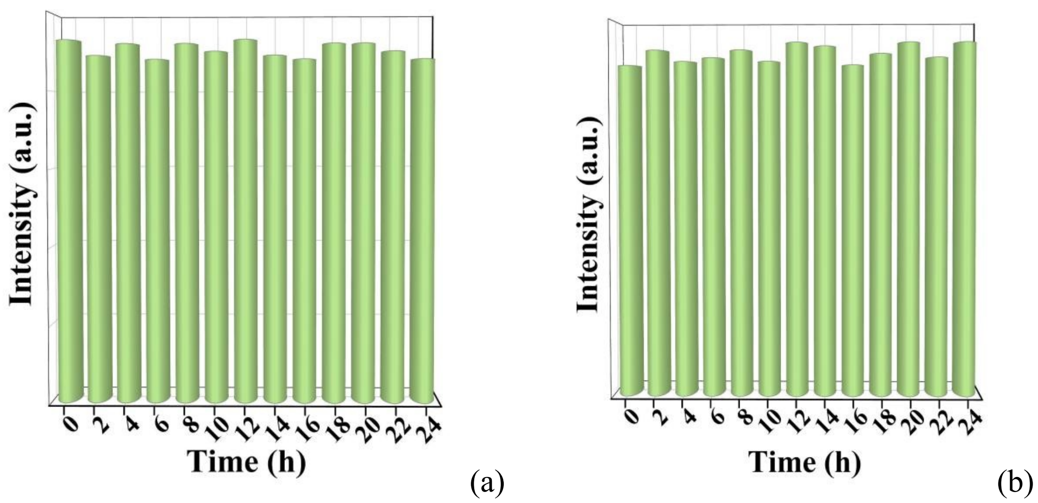

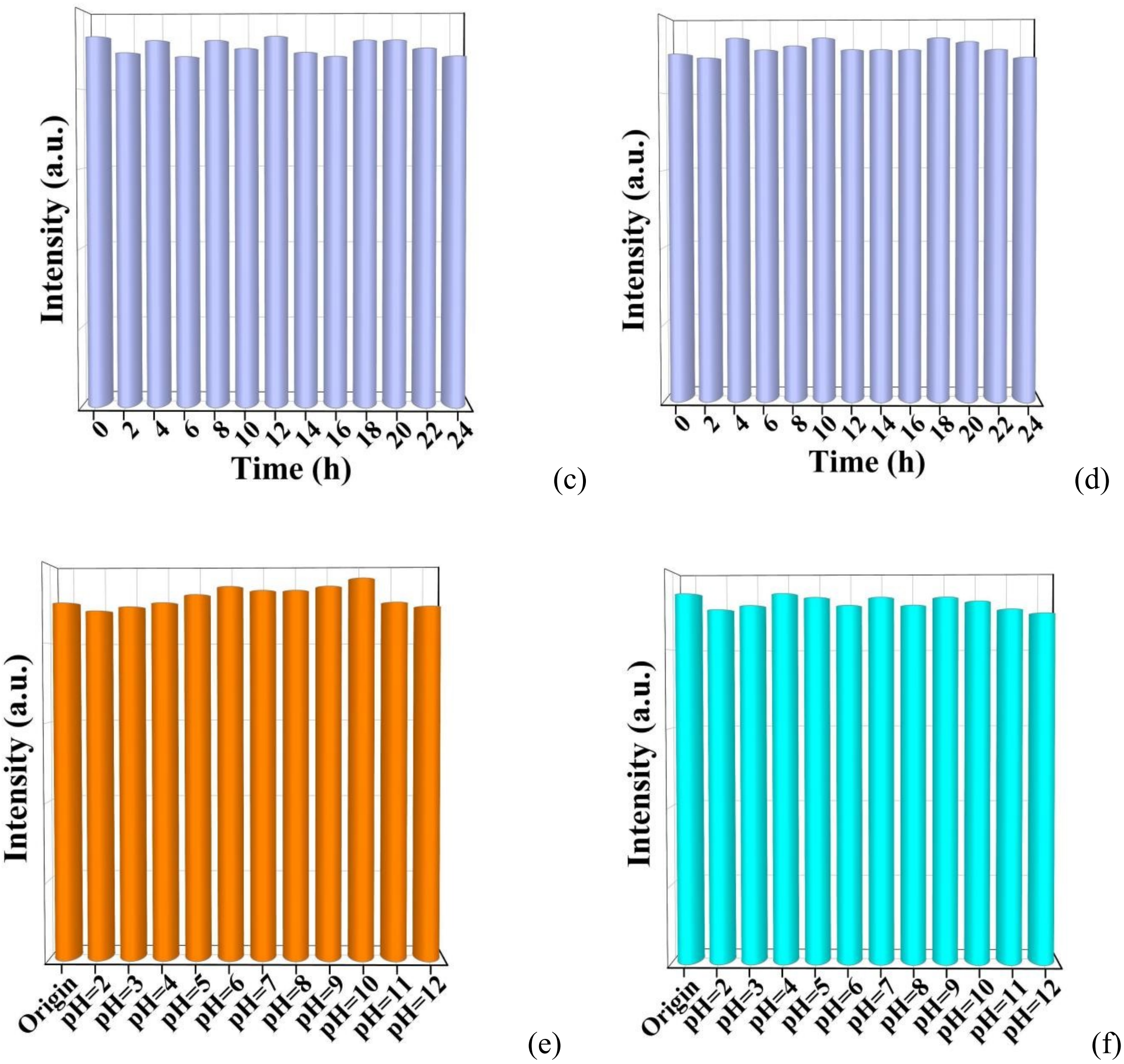

Fig. S6. The fluorescence emission intensities of **1** and **2** in water (a) and (b), EtOH (c) and (d), and different pH (e) and (f).

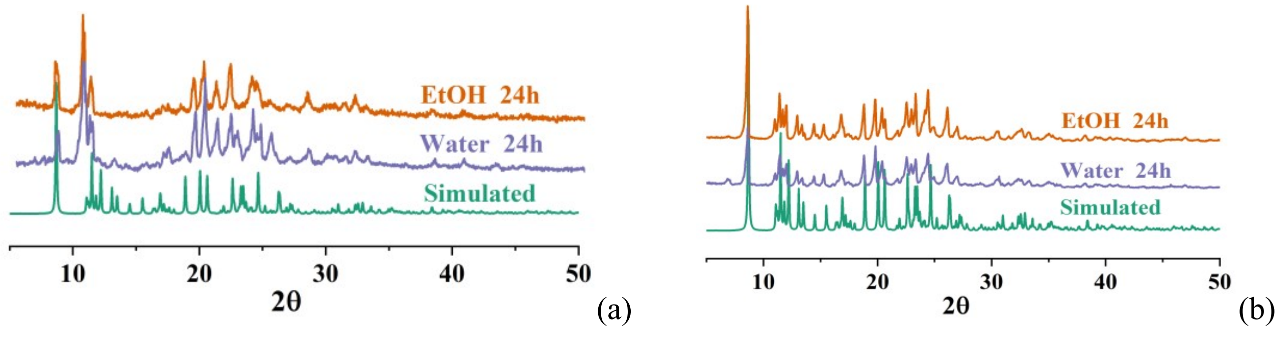

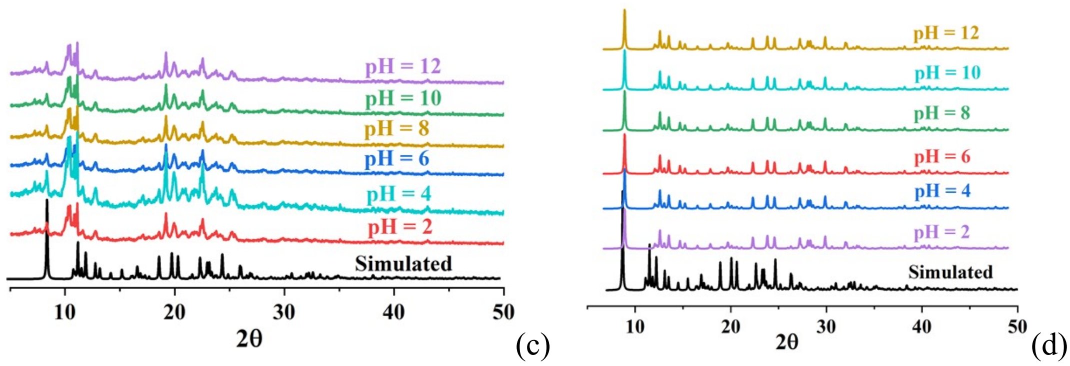

Fig. S7. (a) and (b) PXRD patterns of **1** and **2** after 24h in water and EtOH. (c) and (d) PXRD patterns of **1** and **2** in different pH values.

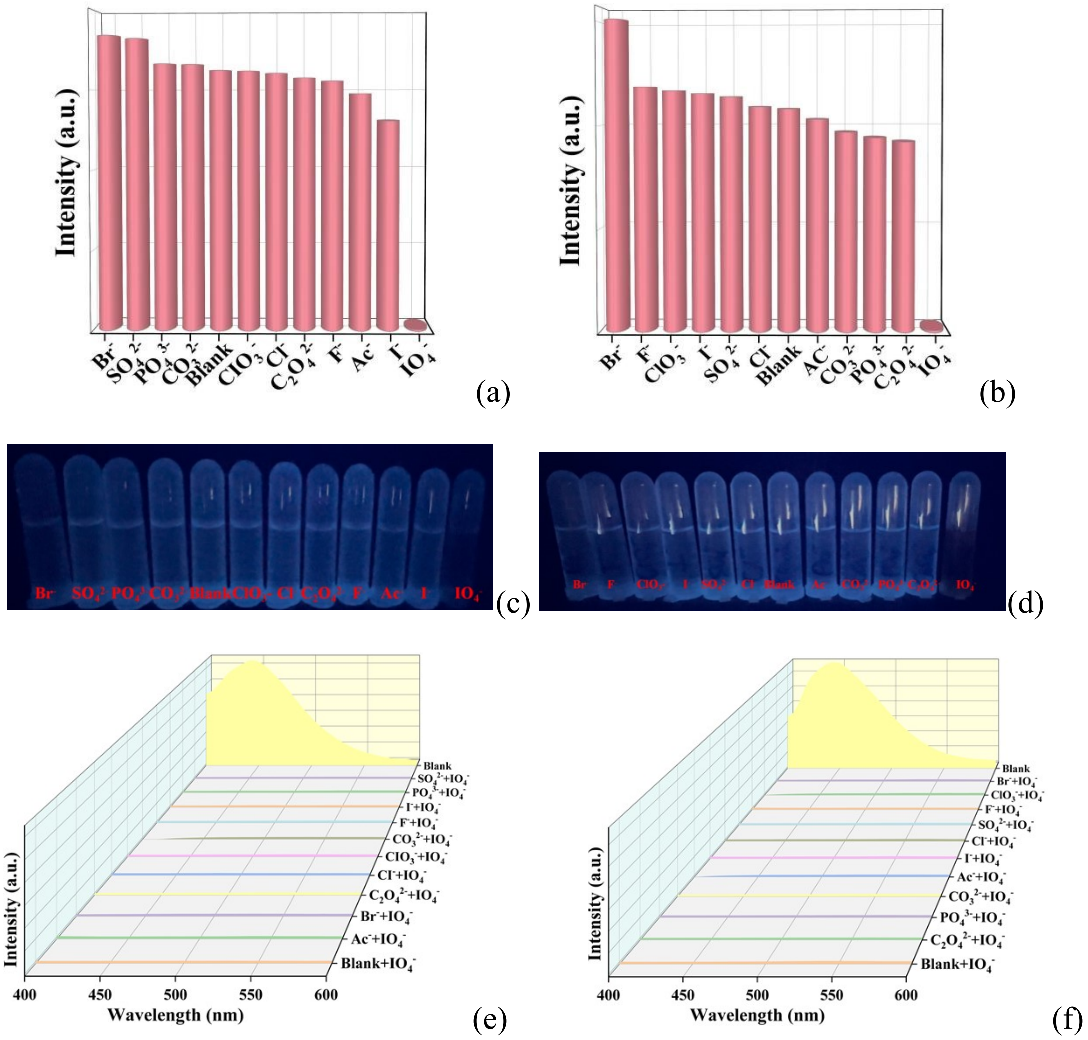

Fig. S8. (a) and (b) Emission intensities of **1** and **2** in different anions aqueous solutions, as well as the corresponding photographs under 365 nm UV light (c) and (d). (e) and (f) Fluorescence responses of IO_4^- for **1** and **2** coexisting with other anions.

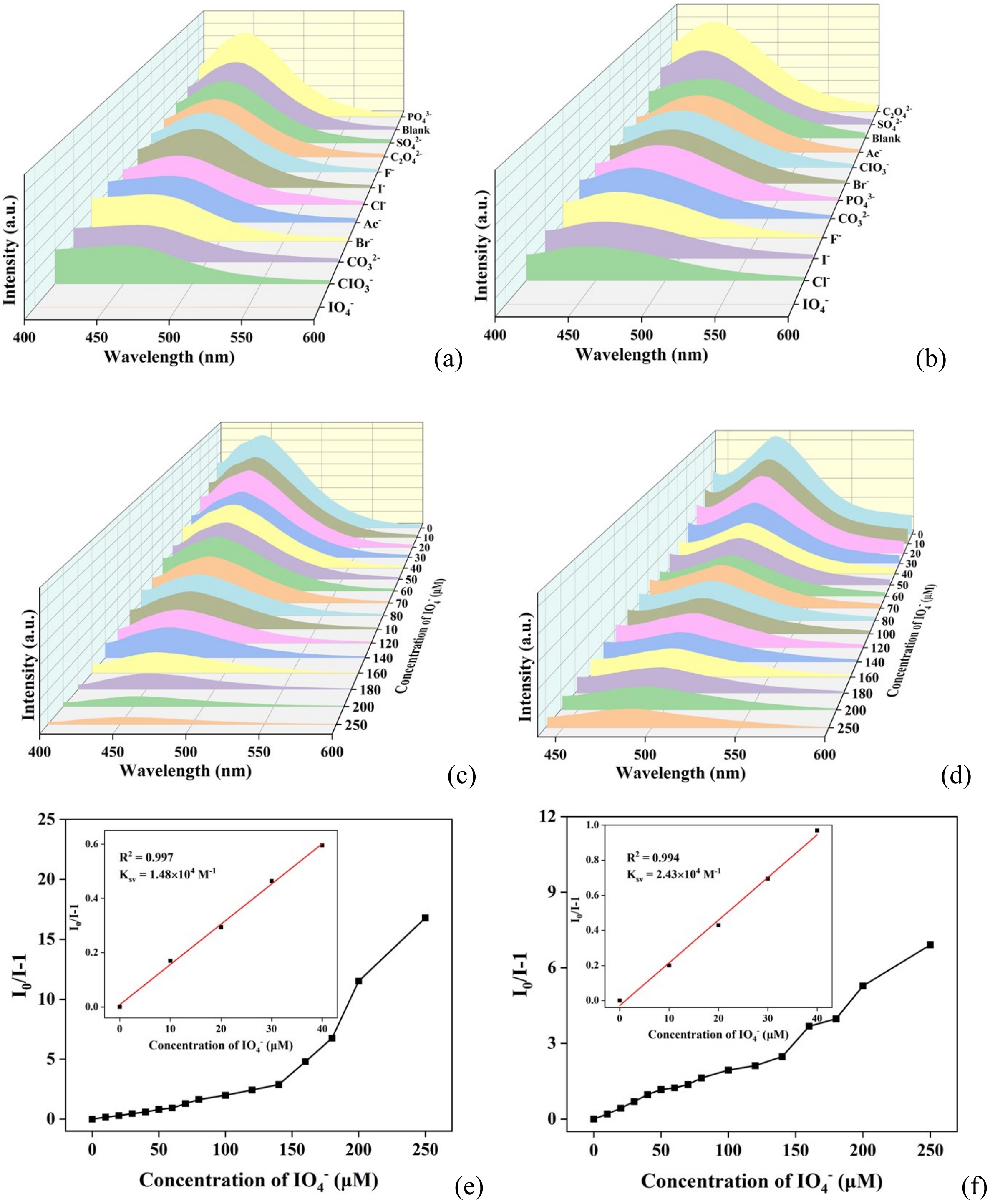

Intensity (a.u.)
Wavelength (nm)
PO4 3-
Blank
SO4 2-
C2O4 2-
F-
I-
Cl-
Ac-
Br-
CO3 2-
ClO3-
IO4-
(a)
(b)
Concentration of IO4- (μM)
(c)
(d)
I0/I-1
R2 = 0.997
Ksv = 1.48×10^4 M-1
(e)
R2 = 0.994
Ksv = 2.43×10^4 M-1
(f)

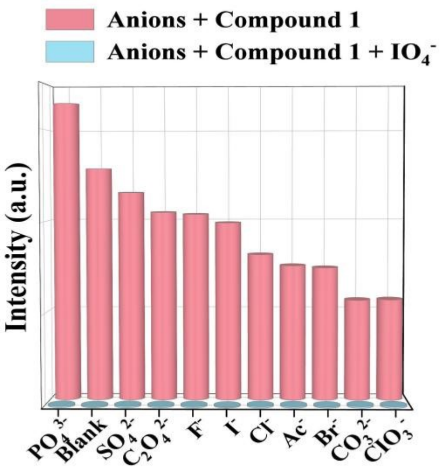

(g)

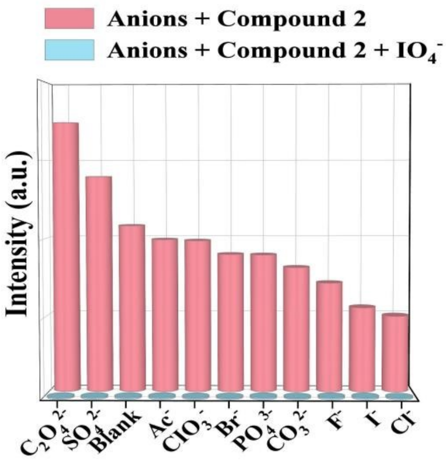

(h)

Fig. S9. (a) and (b) Emission response of **1** and **2** toward anions in swimming pool water. (c) and (d) Emission spectra of **1** and **2** at different concentrations of IO_4^- in swimming pool water suspensions. (e) and (f) The S-V plots of **1** and **2** toward IO_4^- in swimming pool water. (g) and (h) Anti-interference responses for **1** and **2** toward IO_4^- in the presence of other anions.

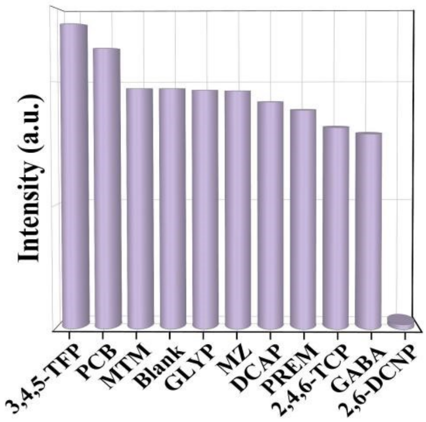

(a)

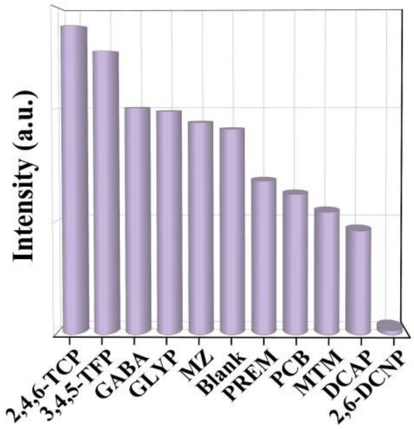

(b)

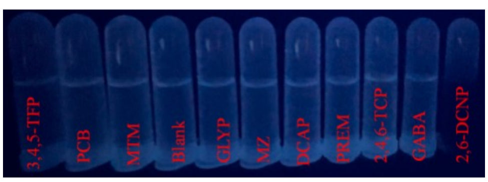

(c)

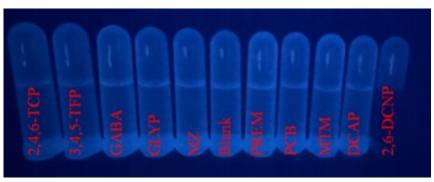

(d)

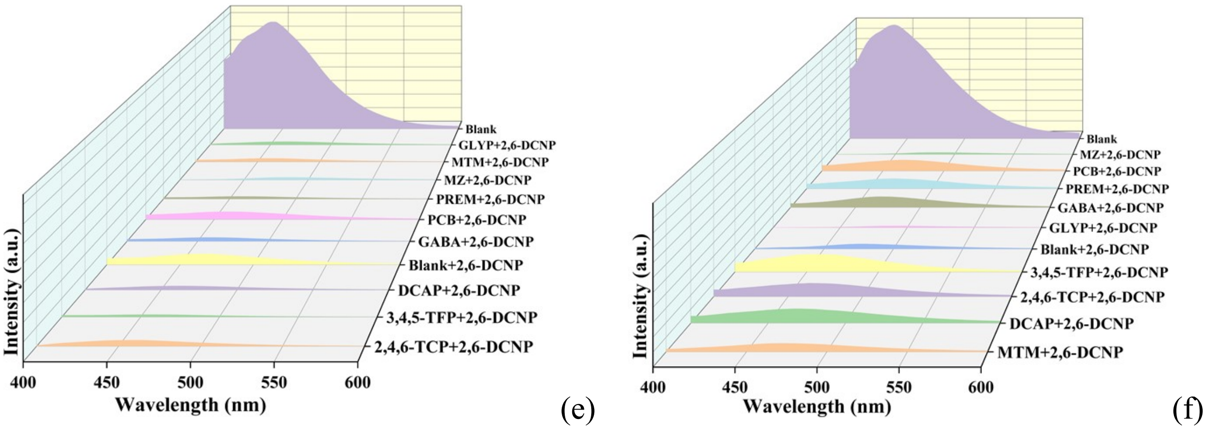

Fig. S10. (a) and (b) Emission intensities of **1** and **2** in EtOH solutions of different agricultural chemicals, as well as the corresponding photographs under 365 nm UV light (c) and (d). (e) and (f) Fluorescence responses of 2,6-DCNP for **1** and **2** coexisting with other agricultural chemicals in EtOH.

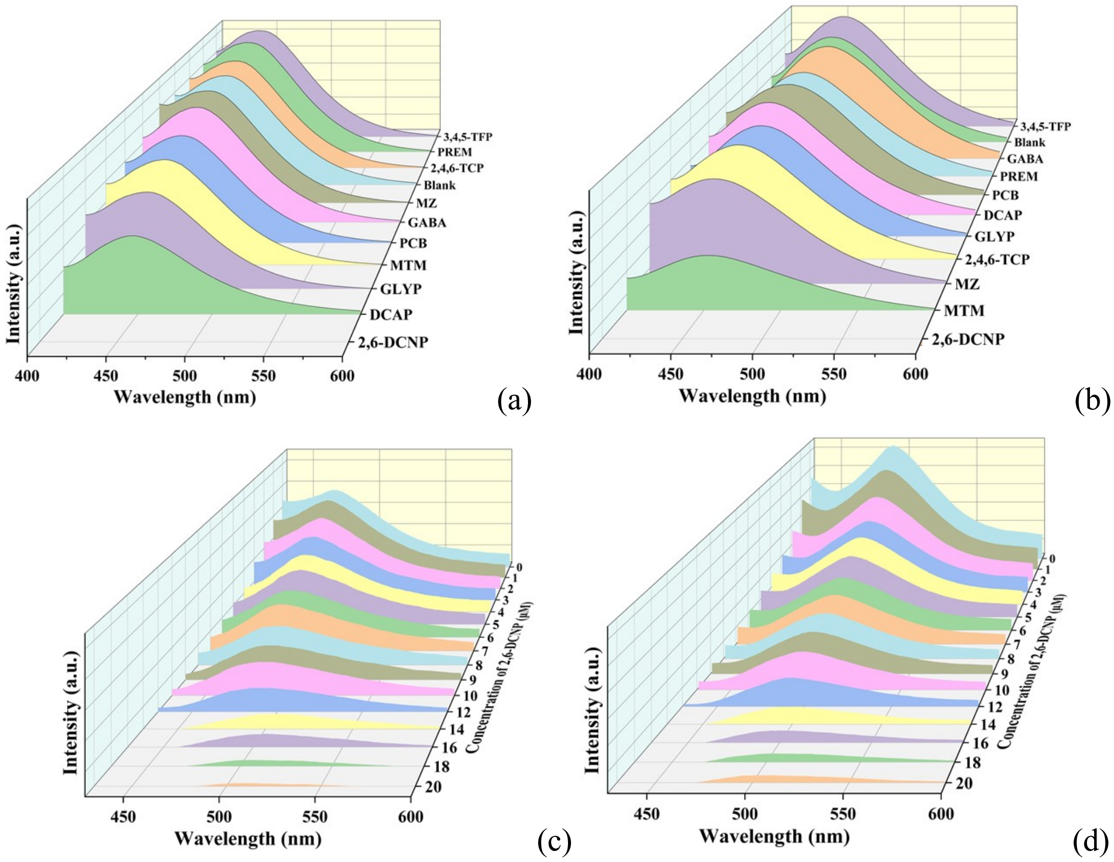

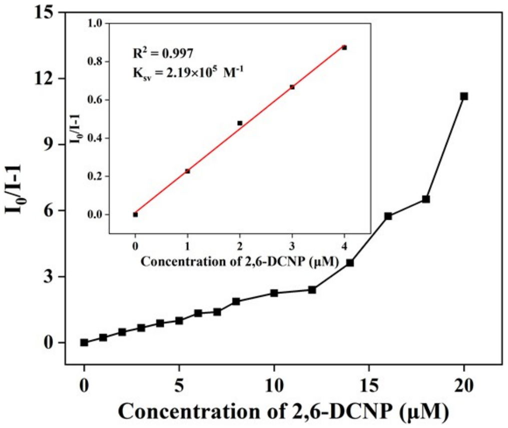

(e)

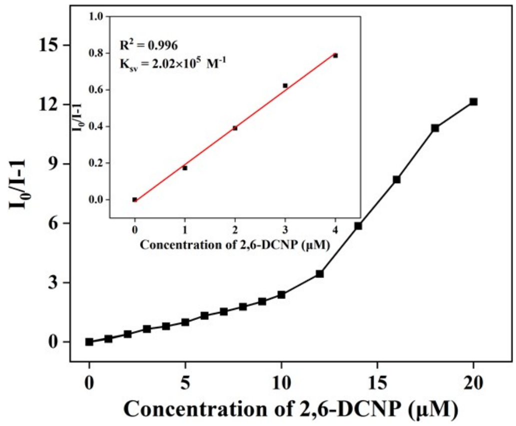

(f)

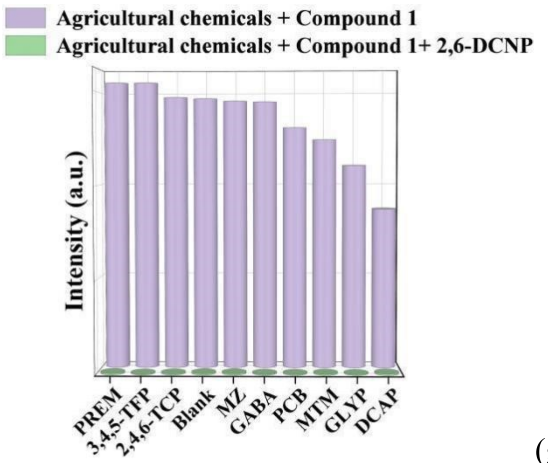

(g)

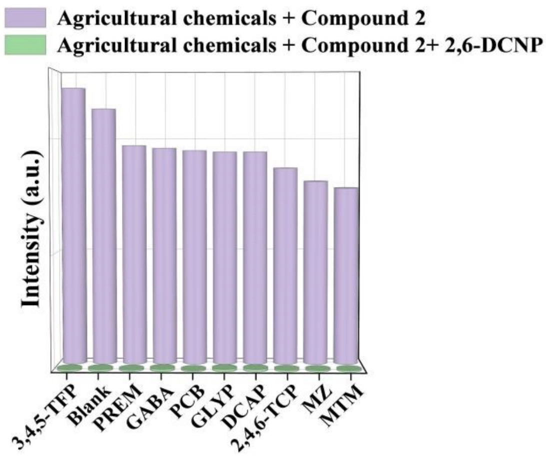

(h)

Fig. S11. (a) and (b)Emission response of **1** and **2** toward 2,6-DCNP in farmland sewage. (c) and (d) Emission spectra of 1 and 2 at different concentrations of 2,6-DCNP in farmland sewage. (e) and (f) The S-V plots of **1** and **2** toward 2,6-DCNP in farmland sewage. (g) and (h) Anti-interference responses for **1** and **2** toward 2,6-DCNP in the presence of other anions.

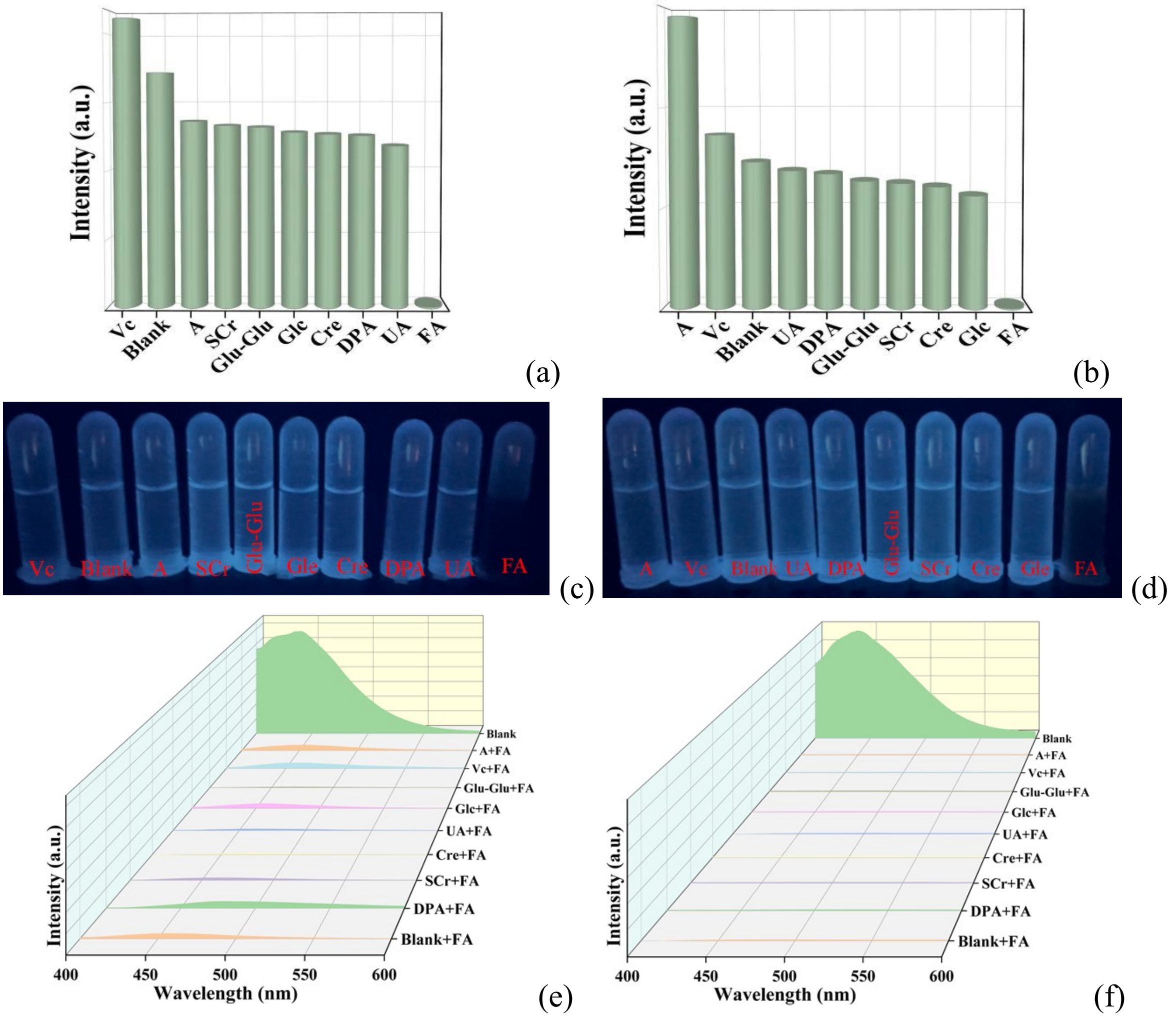

Fig. S12. (a) and (b) Emission intensities of **1** and **2** in aqueous solutions of different biological analytes, as well as the corresponding photographs under 365 nm UV light (c) and (d). (e) and (f) Fluorescence responses of FA for **1** and **2** coexisting with other biological analytes in water suspensions.

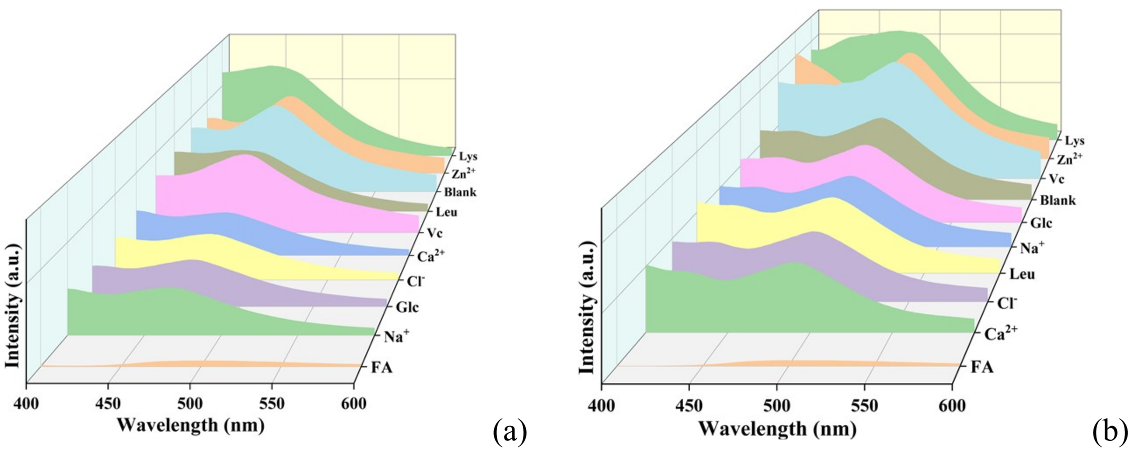

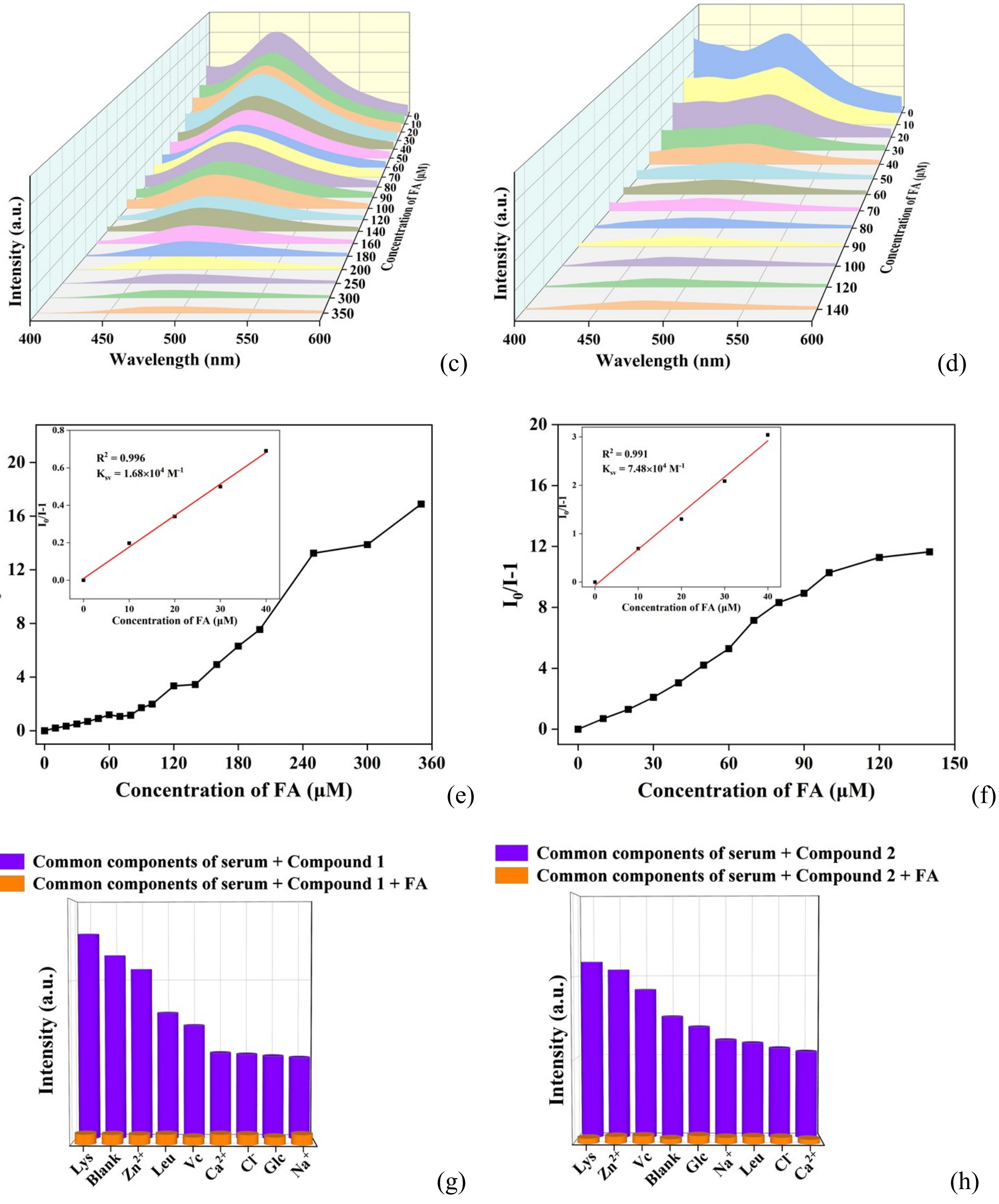

Fig. S13. (a) and (b)Emission response of **1** and **2** toward various biological analytes in serum. (c) and (d) Emission spectra of **1** and **2** at different concentrations of FA in serum. (e) and (f) The S-V plots of **1** and **2** toward FA in serum. (g) and (h) Anti-interference experiment with the addition of FA solution to other biological analytes.

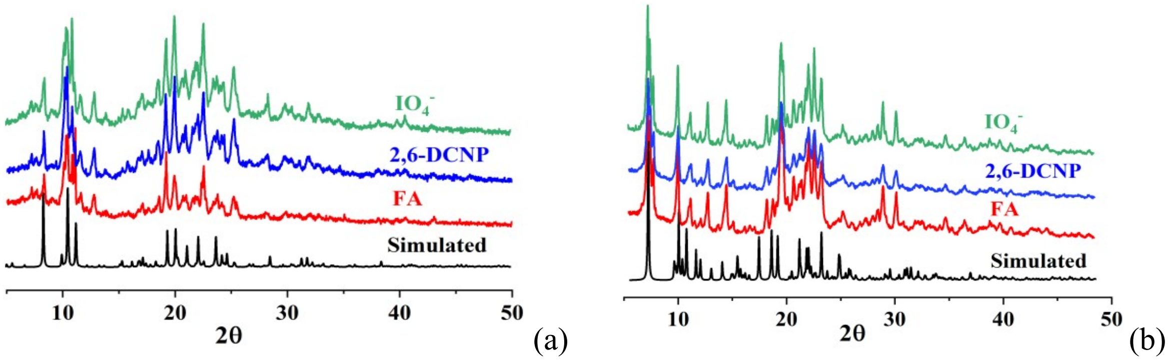

Fig. S14. PXRD patterns of 1 and 2 after the detection.

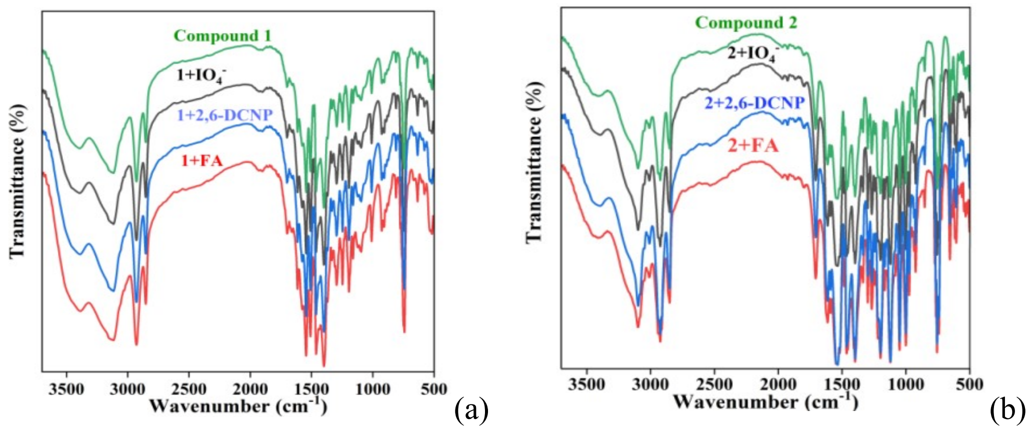

Fig. S15. IR spectra of **1** and **2** after the detection.

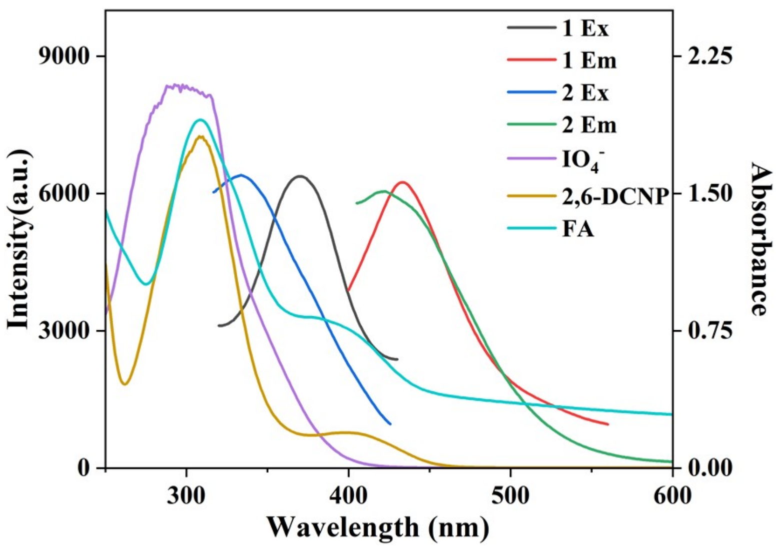

Fig. S16. The overlap of the UV-vis spectra of IO_4^-, 2,6-DCNP and FA with the excitation or emission spectra of **1** and **2**.

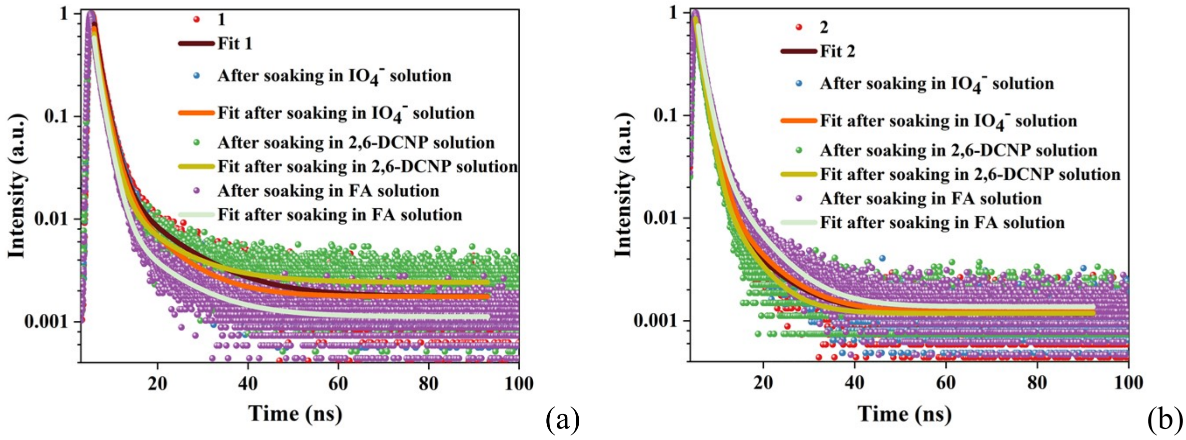

Fig. S17. Fluorescence lifetimes of **1** and **2** before and after addition of the analytes.

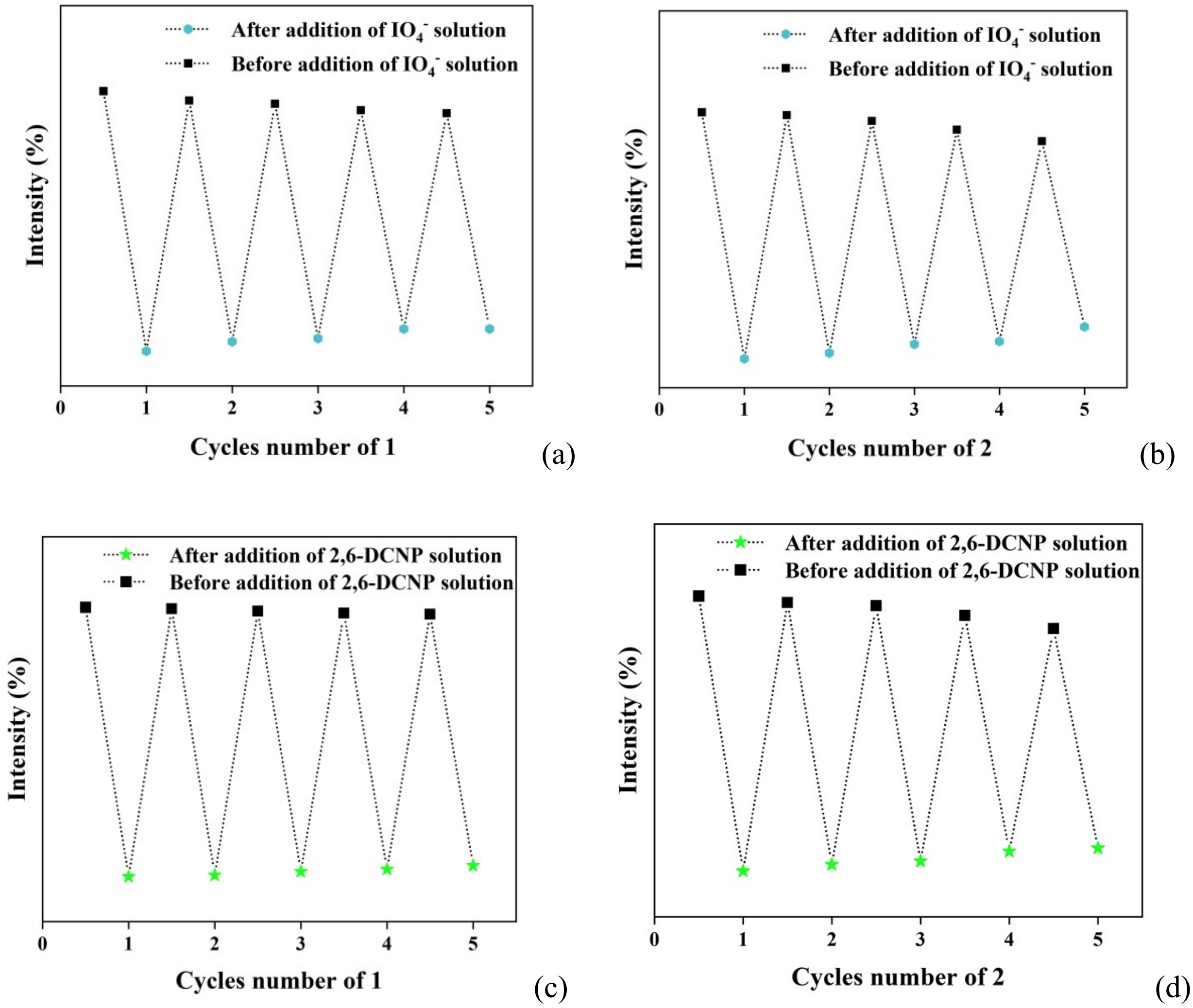

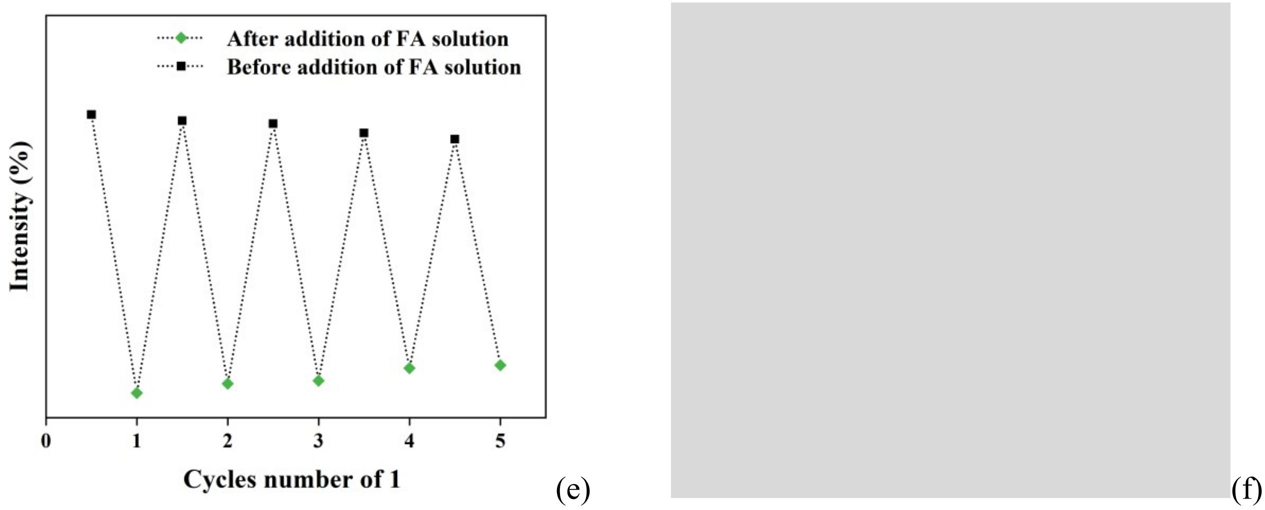

Fig. S18. The fluorescence intensity of **1** and **2** after five cycles of the experiment.

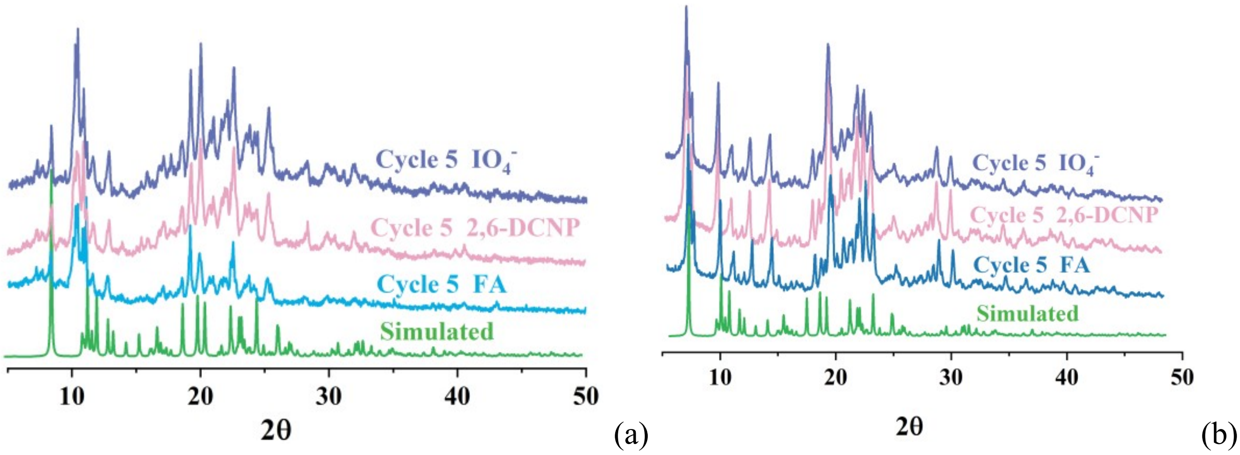

Fig. S19. PXRD patterns of **1** and **2** after five cycles of the experiment.

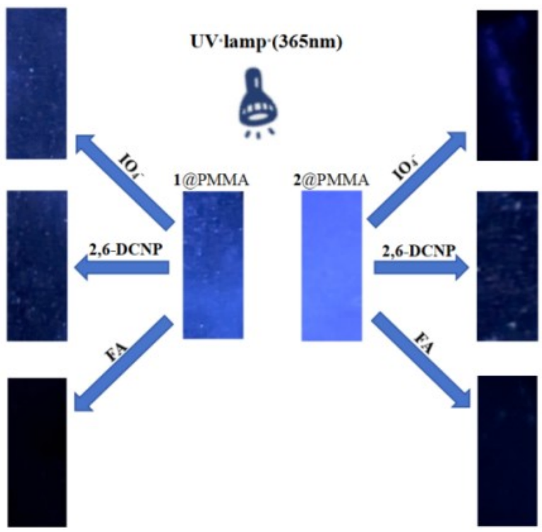

Fig. S20. The films of **1** and **2** toward IO_4^-, 2,6-DCNP and FA under 365 nm UV lamp.